in the deep layer of MT (+1.4±3.9 ms, p=0.10) and cMF (+1.9±5.4ms; p=0.11) and tended to decrease in the LFTC, (Table); however, a significant reduction was only observed in the superficial layer of the cLF (-1.1±2.1 ms, p=0.03 without adjusting for multiple comparisons).Non-progressor knees maintained their MFTC cartilage thickness over the one-year period (+22±72μm) and in these knees, cartilage T2 tended to decrease in both the MFTC and LFTC; however the changes did not reach statistical significance (p≥0.05, Table).
Further, longitudinal (1-year) change in T2 times did not differ significantly between progressors and non-progressors (Table), although cartilage thickness change did (p <0.001 in MT and cMF). The differences in longitudinal change in the deep layer of MT and cMF, however, were close to reaching statistical significance (p=0.05 and p=0.06, respectively).
Conclusions: This is the first study analyzing cartilage T2 in OA knees with subsequent structural progression and non-progressive controls. A limitation is the small sample size, but strengths are that progressors and non-progressors were selected from a relatively large sample of OA knees using two independent methods (MRI and radiography), and that these were matched 1:1 with controls based on radiographic disease stage and demographic characteristics. The results are not suggestive of cartilage T2 in either the deep or superficial layer predicting structural progression in the same compartment. Further, only relatively mild differences were seen in the longitudinal rates change of cartilage T2 between progressors and non-progressor knees, despite dramatic differences in medial cartilage loss between both groups. Future work will explore whether differences in cartilage T2 beween progressor and non-progressor knees become more obvious when extending the analysis to a larger sample.

337
ESTABLISHING A NON-HUMAN PRIMATE MODEL OF OSTEOARTHRITIS USING TRANSLATIONAL ENDPOINTS

M. Wald †, P. Chandran †, G. Tao ‡, R. Tang ‡, D. Conlon §, E. Sampson §, M. Honore †, R. Kamath §, S. Wang †, J. Medema †, J. Li †, G. Fox †, Y. Luo †. † *AbbVie Inc., North Chicago, IL, USA;* ‡ *Wincon TheraCells Biotechnologies, Nanning, China;* § *AbbVie Inc, AbbVie Bioresearch Ctr., Worcester, MA, USA*

Purpose: Current animal models of osteoarthritis (OA) have somewhat limited translation value for developing disease-modifying OA drugs (DMOADs) due to species and assessment related mismatches from clinical OA. Here, we investigated the potential of a nonhuman primate (NHP) surgical model of OA as a translational model by characterizing longitudinal arthritic changes using quantitative and semi-quantitative magnetic resonance imaging (MRI) scoring, serum biomarkers, pain behavior tests and histology.
Methods: Six *Cynomolgous macaques* underwent surgical excision of the right knee medial meniscus (MMT) and four age-/weight-matched sham animals served as controls. MRI of the right knee joint were performed longitudinally prior to surgery and at one, two, and four months after surgery on a 3T Phillips MRI scanner using high resolution T_1- and T_2-weighted protocols, and a dynamic contrast enhanced series. Tibial and femoral cartilage plates were manually segmented and divided into subregions for quantitative cartilage assessment. The semi-quantitative MRI Osteoarthritis Knee Scoring (MOAKS) system was used to assess the structural changes of the knee joint, and the uptake of Gd-DTPA contrast agent was quantified in the regions of synovial tissue. OA related pain behaviors including Von-frey, knee flexion, and activity monitoring were assessed using the same time schedule. Blood samples were taken every two weeks to assess serum levels of CTX-1, HA, C2C, and MMP3. Animals were sacrificed at four (3 MMT, 2 sham) and six months (the remainder) post-surgery for histological evaluation of cartilage degeneration, bone alterations, and synovial inflammation. Group differences between MMT and sham were evaluated by a linear mixed model of the change from baseline for the behavioral, cartilage morphometry, and contrast enhancement rate measurements. Wilcoxon rank sum test was used for MOAKS evaluation. Group differences in histological assessments and biochemical biomarkers were analyzed by ANOVA.
Results: Quantitative cartilage analysis depicted significantly thinner cartilage in the posterior medial femur of MMT animals at all timepoints (p<0.0001) and in the central medial tibiofemoral compartment at two months post surgery (p<0.05). Based on MOAKS scores, MMT animals had more cartilage degradation than sham in the central medial tibia at all timepoints (p<0.01) and in the central medial femur at one month (p<0.05) post-surgery. Hoffa-synovitis and whole knee effusion/synovitis scores were significantly higher in the MMT group with the maximal difference occuring at three months post-surgery (p<0.01) and abating thereafter. Higher contrast uptake rate was observed in multiple subregions of synovial tissue (p<0.01) of MMT animals compared to sham, peaking at two months post-surgery. Histological analysis captured increased tibial and femoral medial cartilage degradation in the MMT group relative to sham (p<0.05) with pronounced osteophytes in all MMT animals. MMT animals demonstrated decreased mobility relative to sham post-surgery (p<0.05). No significant differences were detected in other behavioral measures or in any serum biomarkers tested.
Conclusions: In this study, MRI joint assessment demonstrated cartilage loss and synovial inflammation, both hallmarks of OA progression. These findings coupled with reduced physical activity and histological confirmation of OA-specific pathology are the first reported findings in a NHP model of surgically-induced OA. Additional assessment of this model with pharmacological intervention will further elucidate the utility of this novel translational platform for the development of DMOADs.

338
CORRELATION BETWEEN 3D JOINT SPACE WIDTH ON STANDING CT AND WORMS CARTILAGE MORPHOLOGY

N. Segal †, E. Frick ‡, M. Nevitt §, J. Torner ‡, D. Felson ‖, A. Guermazi ‖, D. Anderson ‡. † *The Univ. of Kansas, Kansas City, KS, USA;* ‡ *The Univ. of Iowa, Iowa City, IA, USA;* § *Univ. of California, San Francisco, San Francisco, CA, USA;* ‖ *Boston Univ. Sch. of Med., Boston, MA, USA*

Purpose: Due to plain radiographs acquiring 2D images of a 3D structure, patient positioning has a large impact on the apparent JSW, and the resulting variations can cause substantial imprecision in measurements. Overlapping bony structures on 2D images make JSW measured from plain radiographs insensitive_approximately 45% of knees with at least partial-thickness cartilage loss are graded as “completely normal.” 3D images acquired using a low-dose standing CT (SCT) scanner are unencumbered by overlapping anatomy, potentially improving concurrent validity with MRI and obviating the need for separate radiographic acquisitions at multiple beam angles. If JSW from SCT accurately represents cartilage morphology, the cost and duration of knee OA clinical trials may be reduced through enabling recruitment of people with known disease status and more sensitive evaluation of outcomes. The purpose of this study was to assess the association between medial tibiofemoral JSW measured on 3D SCT and WORMS cartilage morphology scores.
Methods: This study was conducted ancillary to the 84-month visit of the Multicenter Osteoarthritis Study (MOST), an NIH-funded longitudinal observational study of community-dwelling men and women with or at risk for knee osteoarthritis. Participants at the Iowa site were eligible if they had bilateral, standing fixed-flexion knee radiographs in the prior 6 months, knees discordant for KL grade and with KL<4 (to include a range of JSW) and a distal thigh width on PA radiographs that did not exceed the 38.1cm SCT gantry width. Out of 83 participants who met inclusion criteria, the first 20 volunteers were enrolled. For SCT, a commercial scanner (PedCAT, Curvebeam LLC, Warrington, PA) was modified to enable imaging of bilateral knees in a standing fixed-flexion configuration. A custom radiolucent positioning system was used to maintain foot external rotation and fixed knee flexion angles. The scanner produced pulsed cone-beam x-ray (effective dose equivalent 0.1 mSv) on a 30x30 cm amorphous silicon flat-panel detector (0.194mm pixel size) over a 360° projection angle. A 3D axial CT dataset was reconstructed from initial cone-beam projection images, and bones were segmented in a semi-automated manner. Medial tibiofemoral JSW was assessed on fixed flexion SCT by measuring the intra-articular closest distances between points on the tibiofemoral bony articular margins (Figure 1). Knee MRI was completed using a 1-Tesla ONI OrthOne extremity MRI scanner (GE Healthcare, Waukesha, WI). Experienced radiologists assessed the medial tibiofemoral cartilage morphology on axial and sagittal proton-density weighted fat-suppressed (PDFS) fast spin echo sequences and a coronal STIR sequence, using the WORMS system (0-6). The associations between the percent articular surface area with JSW <2.5mm and the WORMS-CM scores for the central medial tibia and femor were assessed using Spearman's rho, including one randomly selected knee per participant to avoid intra-participant covariance between limbs. A sensitivity analysis, using the

area with JSW <3.0mm was conducted to assess for consistency of the relationship between 3D JSW and WORMS-CM.
Results: Out of the 40 knees, 7 either could not be validly segmented or had no joint space. For the 19 participants included (33 knees), mean±SD age was 66.9±5.4, BMI was 29.5±4.4, 42.1% were female and KL grades were 0 (21.2%), 1 (36.4%), 2 (18.2%), and 3 (24.2%). The % area with JSW<2.5mm correlated with WORMS-CM scores for the central medial tibia (r=0.84, p<0.0001) and central medial femur (r=0.60, p<0.0001). Sensitivity analysis found no significant differences when using the % area with JSW<3.0mm, with correlations of (r=0.82, p<0.0001) and (r=0.62, p<0.0001) respectively. Figure 2 depicts JSW for all 33 knees and the respective central medial tibial WORMS-CM scores.
Conclusions: Greater surface area with a low JSW, as determined by SCT, correlates strongly with the presence and severity of partial and full thickness cartilage lesions in the medial tibiofemoral subregions as determined by semi-quantitative MRI.

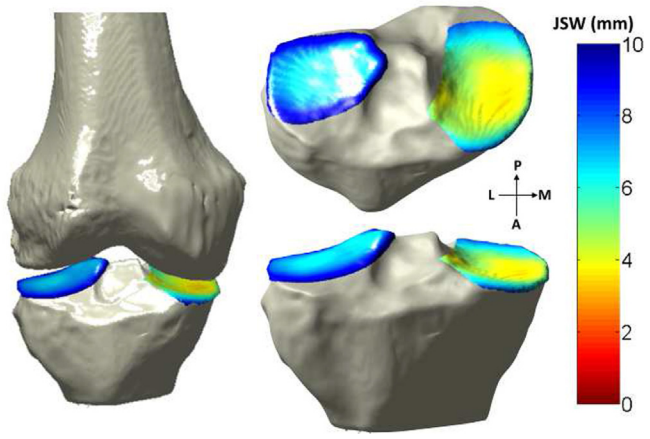

Figure 1. Tibiofemoral Joint Space Width.

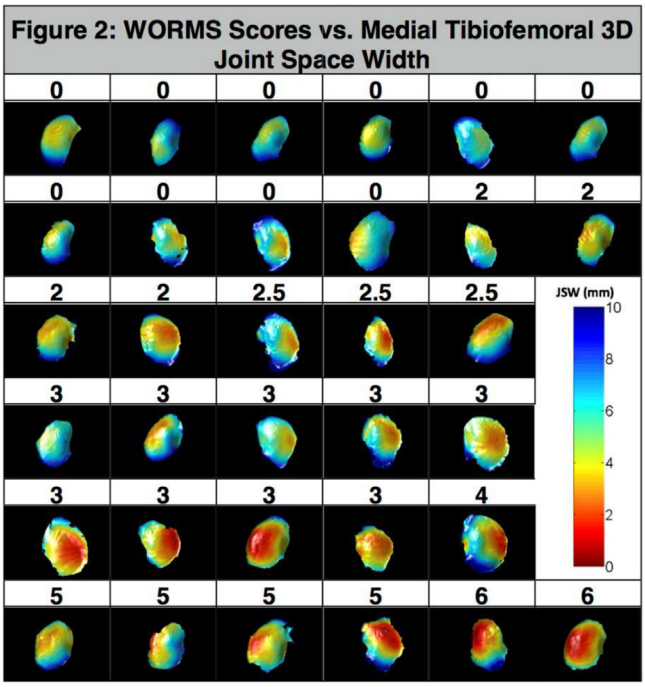

Figure 2. WORMS Scores vs. Medial Tibiofemoral 3D Joint Space Width.

339
RESPONSIVENESS OF INFRA-PATELLAR FAT PAD (IPFP) VOLUME CHANGE WITH SEVERE BODY WEIGHT GAIN AND LOSS – DATA FROM THE OAI

E. Steidle-Kloc, T. Dannhauer, W. Wirth, F. Eckstein. *Inst. of Anatomy, Paracelsus Med. Univ. Salzburg & Nuremberg, Salzburg, Austria*

Purpose: Obesity is an important risk factor of knee OA. Its effect has been suspected to be partly conveyed by endocrinological mechanism, with fat cells secreting (pro-) inflammatory cytokines. The infra-patellar fat pat (IPFP) has raised recent interest, in this context, as it represents an accumulation of intra-articular adipose tissue, a source of intra-articular leptin (and other "adipokines"), and hence a potential mediator of intra-articular inflammation. However, to what extent IPFP morphology is responsive to weight gain or loss is unknown. The purpose of this study therefore was to investigate whether IPFP volume is "responsive" to ≥20% weight gain or loss during 2-year longitudinal follow-up. We further explored whether volumetric analysis of the IPFP is superior (i.e. more sensitive to weight change) than single slice analysis.
Methods: We studied the right knee of all of the 4,796 Osteoarthritis Initiative (OAI) participants who a) displayed a ≥20% weight gain or ≥20% weight loss between baseline and 2-year follow-up, and b) maintained at least some of that weight change (≥5%) at 4-year follow-up. In these participants, all slices clearly depicting the IPFP were manually segmented by one reader (E.S.), using a sagittal intermediately weighted fat-suppressed turbo spin-echo images (slice thickness 3.0 mm, in-plane resolution 0.36 mm). The IPFP volume, its anterior surface (towards the lig. patellae), and its mean 3D thickness (depth) were computed using custom software. Further, the software determined the IPFP area in the sagittal image displaying the maximum IPFP area, and in the central segmented sagittal slice. If an even number of slices was segmented, that central slice with the greater IPFP area was used. Within subject changes (baseline →2-year follow-up) were tested for statistical significance using paired t-tests, differentiating between those with weight gain or loss. Change in IPFP volume was considered the primary outcome, and change in anterior surface areas and depth exploratory outcome. The standardized response mean (SRM= mean change/SD change) was used as a measure of sensitivity to change.
Results: There were 10 participants with ≥20% weight gain and 9 with ≥20% weight loss. Those with ≥20% weight gain were 60% female, had a baseline BMI (mean±SD) of 23.2±4.0 kg/m^2 and had an increase in body weight of 30±10%. Those with ≥20% weight loss were 89% female, had a baseline BMI of 33.8±5.3 kg/m^2 and a reduction in body weight of -23±3%.
Surprisingly, in those with weight gain, there was a concurrent -2.6% ((absolute difference in %) volume reduction of the IPFP over the 2 years. This volume change appeared to be more strongly driven by change in anterior surface area (-2.9%) than in IPFP depth (0.4%) but did not reach statistical significance. The SRM of the IPFP volume change was larger than that for single images (Table 1, figure 1).
In those with weight loss, there was a concurrent -4.0% volume reduction of the IPFP over the 2 years. This volume change, again, appeared to be more strongly driven by change in anterior surface area (-6.0%) than in IPFP depth (2.0%) but did not reach statistical significance. As with weight gain, the SRM for IPFP volume changes during weight loss was larger than that for single images (Table 1, figure 1).

Table 1
IPFP morphometric change in 10 OAI participants with ≥20% weight gain.

	Mean ± SD Change	SRM	95% CI Change
IPFP Volume [cm^3]	-0.78±1.52	-0.51	-1.7,0.2
Anterior surface [cm^2]	-0.75±2.30	-0.32	-2.2,0.7
Depth [mm]	0.04±0.70	0.06	-0.4,0.5
IPFP maximal sagittal area [cm^2]	-0.02±1.19	-0.01	-0.8,0.7
IPFP central segmented image [cm^2]	0.24±1.35	0.17	-0.6,1.1

Table 2
IPFP morphometric change in 9 OAI participants with ≥20% weight loss.

	Mean ± SD Change	SRM	95% CI Change
IPFP Volume [cm^3]	-1.11±2.15	-0.52	-2.5,0.3
Anterior surface [cm^2]	-1.53±2.23	-0.69	-3.0,-0.1
Depth [mm]	0.22±0.48	0.46	-0.1,0.5
IPFP maximal sagittal area [cm^2]	0.29±1.30	0.22	-0.6,1.1
IPFP central segmented image [cm^2]	-0.23±1.70	-0.13	-1.3,0.9